

## Original Article

# A novel frameshift mutation in the NMTS domain of RUNX2 in a Chinese family with cleidocranial dysplasia

Ting Chen<sup>1\*</sup>, Ling Peng<sup>1\*</sup>, Mei-Yi Li<sup>2</sup>, Fu-Chun Fang<sup>1</sup>, Ting Lu<sup>1</sup>, Zhao Liu<sup>1</sup>, Fei Liu<sup>1</sup>, Jia-Wen Mo<sup>3</sup>, Ci Song<sup>1</sup>, Fu Xiong<sup>2</sup>, Bu-Ling Wu<sup>1</sup>

<sup>1</sup>Department of Stomatology, Nanfang Hospital, College of Stomatology, Southern Medical University, Guangzhou, China; <sup>2</sup>Department of Medical Genetics, School of Basic Medicine Sciences, Southern Medical University, Guangzhou, China; <sup>3</sup>Department of Biopharmaceutical, School of Biotechnology, Southern Medical University, Guangzhou, China. \*Equal contributors.

Received December 19, 2016; Accepted January 27, 2017; Epub April 1, 2017; Published April 15, 2017

**Abstract:** Cleidocranial dysplasia (CCD) is an autosomal dominant heritable skeletal disorder, caused by heterozygous mutations of *Runx2*. This study aimed to investigate the *Runx2* mutation in a Chinese family with CCD and study the pathogenesis of the mutational *Runx2* gene. A 29-year-old male was diagnosed as proband of CCD based on the clinical findings, which show hypoplastic clavicles, underdeveloped maxilla, supernumerary teeth, and retention of deciduous dentition. Sanger sequencing showed the presence of a novel deletion mutation, c.1271delC, in exon 7 within the nuclear matrix targeting signal domain of the proband's *Runx2* gene. We did not find any mutations in the unaffected family members or 200 healthy random individuals. In vitro analysis revealed significantly increased expression of the p.P424HfsTer39 variant at the protein level compared to wild-type RUNX2 protein. The study of the Green fluorescent protein fusion indicated that the 1271delC mutation affected the nuclear accumulation of RUNX2 protein. The findings showed that the 1271delC introduced a novel stop codon at codon 483, which had caused a truncated RUNX2 protein and impaired subcellular localization of RUNX2, resulting in CCD pathogenesis. The results broaden the spectrum of the mutation in the *Runx2* gene and offer the new evidence to study the pathogenesis of *Runx2* gene mutations.

**Keywords:** Cleidocranial dysplasia, Runx2, frameshift mutation, NMTS domain, subcellular localization

## Introduction

Cleidocranial dysplasia (CCD) is an autosomal-dominant genetic disease (OMIM119600) that mainly affects the development of bones and teeth with features of familial aggregation, and the clinical incidence rate is approximately 1/1,000,000 [1]. Defected endochondral and intra-membranous bone formation would cause CCD and there were typical clinical symptoms including open sutures and fontanelles, delayed fontanelle closure, hypoplastic clavicles, narrow shoulders, short stature, short and broad thumbs; and oral symptoms such as retention of deciduous teeth, delayed eruption, supernumerary teeth and malocclusion [2]. The heterozygous mutation, deletion and insertion in runt-related transcription factor 2 (*Runx2*) gene would result in the hypomorphic or haploinsufficiency of RUNX2 protein, leading to classic CCD [1, 3].

*Runx2*, located on chromosome 6p21, is necessary for the differentiation of the osteoblast and maturation of chondrocyte [4]. There are eight exons and two promoters (P1 and P2) in the *Runx2*, playing a role in the transcriptional regulation. The type I isoform (regulated by P2), starting with the sequence MRIPV at its N-termini encoded a 507-amino acid protein (NP\_004339.3) and type II isoform (regulated by P1), starting with the sequence MASNS at its N-termini encoded a 512-amino acid protein (NP\_001019801.3). In addition, RUNX2 protein mainly has several function domain as follows: the transactivation domains-glutamine/alanine rich domain (Q/A) and proline/serine/threonine-rich domain (PST); DNA-binding domain-runt homology domain (RHD); domains related to the subnuclear localization-nuclear localization signal (NLS) and nuclear matrix targeting signal (NMTS); repression domain-VWRPY region [5]. The *Runx2* mutation in CCD can

## A novel mutation of RUNX2 in a Chinese family

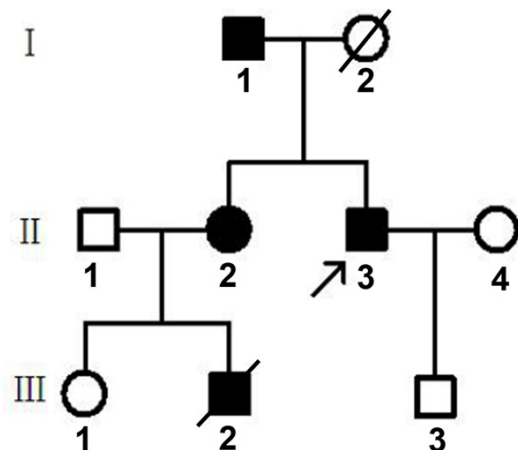


**Figure 1.** Pedigree of the affected family. Black symbols indicate patients with CCD. The arrow indicates the proband.

occur in any domains mentioned above, while it is mostly clustered in the RHD in CCD [6-11]. In the identified mutations, 63% were detected in the RHD and just 20% were in the C-terminus of the RHD and in the RHD, most are missense mutations, which is quite different from the C-terminal mutation, among which missense mutations only account for 10%. The C-terminus of RUNX2 accounts for over 56% of the coding region, but the reported mutations in the region are only 23%. The C-terminus of RUNX2 might bear certain degrees of missense changes, and will not show obvious phenotype of CCD unless there is disruption of large part of generating protein caused by nonsense mutations, frameshift, or splice-site, which will severely interfere the protein structure [12]. NMTS, a segment of 27 to 38 amino acids in the C-termini of RUNX family members, directs RUNX2 to the subnuclear locations, and it is also essential to appropriately regulate downstream target like osteocalcin [13]. Animal experiments have demonstrated that homozygous mice, lacking in the NMTS and C-terminal residues, showed absence of bone tissues due to the loss of osteogenic capability. A mutation or loss of NMTS would affect the size and structural arrangement of protein subnuclear localization [14]. *In vitro* tests have proven that the loss of the NMTS will increase mobility of the protein and cause it to fail to locate in the nucleus [15]. Zhang *et al.* [16] conducted a functional analysis on a nonsense mutation that has been reported many times and found that the truncated RUNX2 protein produced by

the mutation could not complete the transcriptional activation due to loss of the NMTS and other important activation regions, which affected the interaction of RUNX2 with Smad protein.

Although there are continuous reports about the mutation sites of *Runx2* genes in the patients with CCD, the screening of the *Runx2* genes in this disease is far from enough. The identification of the new sites can contribute to the further systematic researches on the mutation and it can also solidify the foundation of the molecular genetics exploring pathogenic mechanism. Here, we describe a novel frameshift mutation within the NMTS domain of RUNX2 in a Chinese family with CCD. *In vitro* functional analysis was conducted to investigate the subcellular localizational ability of the mutant RUNX2 protein.

### Materials and methods

#### *Clinical and radiographic examination of CCD*

A family with the clinical diagnosis of CCD from the Department of Stomatology, Nanfang Hospital, Guangzhou, China, was included in this study (Figure 1). Two calibrated dentists examined and identified the participants suspected of CCD. The proband and other affected family members were received radiographic examinations, including panoramic view, anteroposterior and lateral cephalometric radiographs, chest radiographs, anteroposterior foot and hand radiographs. The diagnosis of CCD was made according to the clinical and radiographic results. The informed consent letters were signed by all the participants and the research was permitted by the Medical Ethics Committee of Nanfang Hospital, an affiliate hospital of Southern Medical University, China.

#### *Mutation screening*

Extraction of genomic DNA from peripheral blood was performed for the family members. Exons 1-7 of the *Runx2* gene and their flanking intronic regions were amplified by polymerase chain reaction (PCR). The PCR primers were designed by primer premier 5.0 (Table 1). The PCR was carried out as follows: 2  $\mu$ L of genomic DNA, 5  $\mu$ L of 10  $\times$  Trans Buffer I, 4  $\mu$ L of dNTPs (10 mM), 0.5  $\mu$ L of DNA Taq Polymerase (Transgene, Beijing, China), 1  $\mu$ L of each primer

## A novel mutation of RUNX2 in a Chinese family

**Table 1.** Primers of RUNX2 for PCR

Exon	Forward Primer	Reverse Primer
Exon 1	TGGCTGTGTGATGCGTATT	GTGGCCTTCAAGGTAAGAGGCTA
Exon 2	CAGATGCTTCATTCTGTC	CTAGTCTGTATACAAATCAGCAC
Exon 3	TCATTGCCTCCTTAGAGATGC	GTTAGTGTCACCTTCATGTCC
Exon 4	AATGCTGGCCACCAGATACCG	GGAGCTGTGAAGCGGCTTATT
Exon 5	TAAGGCTGCAATGGTTGCTAT	CTCATCCATGCTCACAGTGAC
Exon 6	CTCTGGGAAATACTAATGAGG	ATTACAAATGCACATCATGGCACT
Exon 7	TGTGGCTTGCTGTTCT	GCAGTGGCCCAGTGGTATCT

(20  $\mu$ M), made up to 50  $\mu$ L with ddH<sub>2</sub>O. PCR procedure was set by the instruction book and the annealing temperature was set according to the primers. After amplification, the agarose electrophoresis was conducted for the PCR products, and then the products were performed Sanger sequencing at Life Technologies, Inc., Shanghai, China. Sequence comparison was conducted using information in the NCBI database (<http://www.ncbi.nlm.nih.gov>).

### Bioinformatics

Prediction of the three-dimensional (3-D) protein structure of RUNX2 was performed by I-TASSER (<http://zhanglab.ccmb.med.umich.edu/I-TASSER/>); the effect of RUNX2 protein function with P424HfsTer39 mutation was predicted by mutation taster (<http://www.mutationtaster.org/>).

### Population screening

Blood samples were collected from 200 random individuals in the locality of the family, and their genomic DNA was extracted for analysis. We designed the primers, which were 50 bp away from the upstream and downstream ends of the mutational site, as follows: forward 5'-ATGTCCTCGGTATGTCGC-3', reverse 5'-TCCACTCTGGCTTTGGGAAGA-3'. Using high resolution melting technology, we screened the mutation (c.1271delC) to investigate the mutation frequency in the general population.

### RNA analysis in vivo

Total RNA was extracted from affected and unaffected family members. A HiScript™ 1<sup>st</sup> Strand cDNA Synthesis Kit (Vazyme, Jiangsu, China) was used to synthesize complementary DNA. The RNA sequence (transcript variant 1) of RUNX2 was used to design the following RT-PCR primers. Forward 5'-GAACCCAGAAG-

GCACAGACA-3' and reverse 5'-GG-CTCAGGTAGGAGGGGTAA-3'. Real-time RT-PCR was performed using samples from three healthy and three CCD family members to analyze the difference between them in mRNA expression. The GoTaq system (Promega, Madison, WI, USA) relative quantitative RT-PCR was used to measure mRNA from the affected and unaffected individuals. Each 20  $\mu$ L reaction system contained: 100 ng of cDNA, 10  $\mu$ L of 2  $\times$  GoTaq qPCR Master Mix, 0.4  $\mu$ L  $\times$  2 of each primer pair (20  $\mu$ M), made up to 20  $\mu$ L with nuclease-free water. Using Agilent Stratagene Mx3005P Real-Time PCR System (Agilent Technologies, Santa Clara, CA, USA) the reaction process was as follows: 95°C for 3 min, followed by 40 cycles of denaturation at 95°C for 20 s, annealing at 60°C for 30 s and extension at 72°C for 15 s, and then 95°C for 1 min, 55°C for 30 min, and 95°C for 30 s. Gene expression levels were calculated according to the ( $2^{-\Delta\Delta CT}$ ) method. The GAPDH expression level was referred to normalize the expression level of the target gene. Each RT-PCR was repeated for three times and the results of the three times were used for mean values and standard deviation.

GCACAGACA-3' and reverse 5'-GG-CTCAGGTAGGAGGGGTAA-3'. Real-time RT-PCR was performed using samples from three healthy and three CCD family members to analyze the difference between them in mRNA expression. The GoTaq system (Promega, Madison, WI, USA) relative quantitative RT-PCR was used to measure mRNA from the affected and unaffected individuals. Each 20  $\mu$ L reaction system contained: 100 ng of cDNA, 10  $\mu$ L of 2  $\times$  GoTaq qPCR Master Mix, 0.4  $\mu$ L  $\times$  2 of each primer pair (20  $\mu$ M), made up to 20  $\mu$ L with nuclease-free water. Using Agilent Stratagene Mx3005P Real-Time PCR System (Agilent Technologies, Santa Clara, CA, USA) the reaction process was as follows: 95°C for 3 min, followed by 40 cycles of denaturation at 95°C for 20 s, annealing at 60°C for 30 s and extension at 72°C for 15 s, and then 95°C for 1 min, 55°C for 30 min, and 95°C for 30 s. Gene expression levels were calculated according to the ( $2^{-\Delta\Delta CT}$ ) method. The GAPDH expression level was referred to normalize the expression level of the target gene. Each RT-PCR was repeated for three times and the results of the three times were used for mean values and standard deviation.

### RUNX2 protein expression detection in vitro

Human embryonic kidney (HEK) 293 T cells were cultured in DMEM (Invitrogen, Thermo Fisher Scientific, Waltham, MA, USA) with 10% fetal bovine serum (Gibco, Thermo Fisher Scientific). We trypsinized the HEK 293 T cells when they reached the confluence of 80% to 90%, and seeded them in six-well plates for a day to reach the confluence of 80% to 90%. The normal and abnormal transcribed cDNA of the human *Runx2* gene was cloned into the vector pEGFP-C1 (Dingguo Changsheng Biotechnology, Beijing, China), then recombinant wild-type or mutant *Runx2* was transfected into HEK 293 T cells using Lipofectamine 2000 (Invitrogen) according to the manufacturer's instructions. After transfected for 24 h, cells were homogenized in RIPA buffer supplemented with protease inhibitors (Sigma, St Louis, MO, USA) on ice for 30 min. Blotting membranes were incubated with mouse anti-GFP (1:5000, Santa Cruz Biotechnology, Santa Cruz, CA, USA) overnight at 4°C. Next day, blotting

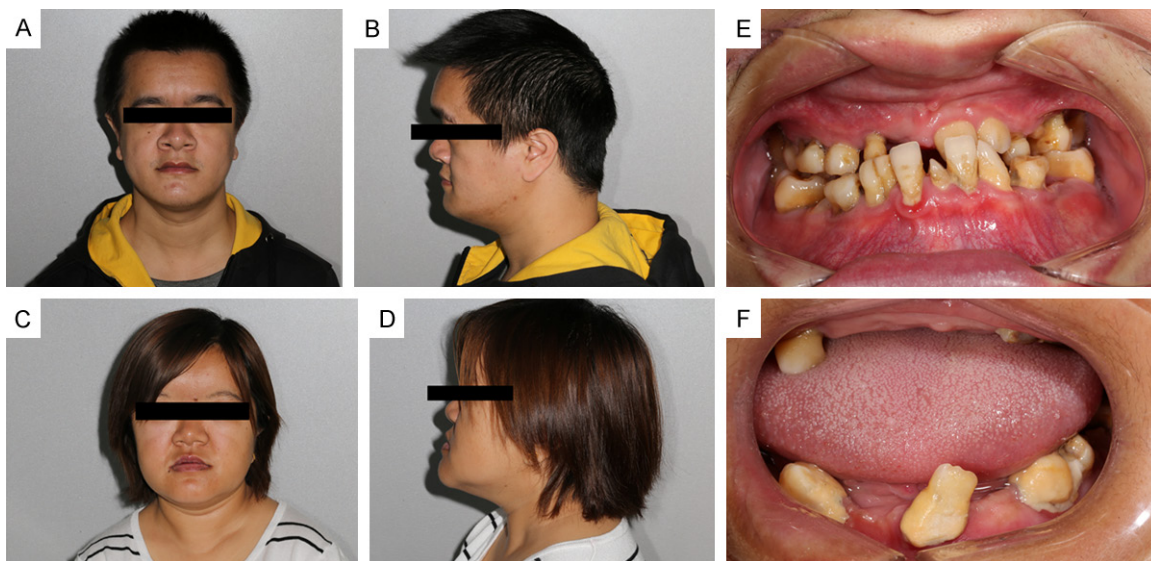


**Figure 2.** Front views, profile and intraoral pictures of the proband and his elder sister. (A-D) Photographs showing the concave mid-face, flattened nose bridge and mandibular protrusion in patients II 3 (A, B) and II 2 (D, E). (E, F) The dental anomalies included malocclusion and deciduous tooth retention in patients II 2 and II 3.

membranes were washed three times and incubated with goat anti-mouse IgG-HRP (1:2000, Santa Cruz Biotechnology) at room temperature for 2 h, then detected with Immobilon western chemiluminescent HRP substrate (Merck-Millipore, Darmstadt, Germany).

#### Cell localization studies

After HEK 293 T cells were transfected for 24 h, medium was removed, and cultures were flushed three times with preheated PBS, 5 min each time. Cell nuclei were counterstained with 4',6-diamidino-2-phenylindole (DAPI; Sigma). Dye development was observed every 5 min under the fluorescence microscope and when complete, cells were changed into fresh culture medium. Photographs were taken under a fluorescence microscope (Nikon, Eclipse Ti-U, Tokyo, Japan) and RUNX2 protein relocation was compared between the wild-type and mutant proteins.

## Results

#### Clinical phenotype of CCD patients

The proband (a 29-year-old male, II 3) has an affected father (70 years old, I 1) and a healthy son (8 years old, III 3). The proband's elder sister had an affected son (died at the age of 6, III 2) and a healthy daughter (12 years old, III 1).

The proband and his elder sister showed a concave mid-face, flattened nose bridge and mandibular protrusion (**Figure 2A-D**). Dental anomalies included unerupted teeth with supernumerary permanent teeth in the maxilla and mandible, malocclusion, retention of deciduous teeth, and eruption failure of permanent teeth (**Figure 2E, 2F**).

Panoramic radiographic examination the roots of unerupted teeth which were basically fully grown and were impacted in the bone, while the roots of deciduous teeth were not absorbed but covered the crown surfaces of unerupted permanent teeth in the proband (**Figure 3A**) and his elder sister (**Figure 3B**), and the supernumerary teeth were located in the bilateral premolar regions in the proband. Besides, the narrow ascending ramus, with near parallel-sided anterior and posterior borders could be discovered evidently. The proband also had other craniofacial and skeletal abnormalities. Craniofacial features (**Figure 3C, 3D**) included underdeveloped maxilla and nasal bone, wormian bones in the occipital bone. Other skeletal features (**Figure 3E-G**) included hypoplastic or aplastic bilateral clavicles, mitri-form thoracic cage, and shortened distal phalanges of both thumbs and toes. Typical dental and skeletal features could be seen both in the other two affected individuals and in the proband. In all, the diagnosis of CCD could be sup-



**Figure 3.** Panoramic radiographs of the proband and his elder sister. And other radiological findings of the proband. (A, B) Panoramic view showing the roots of unerupted teeth which were basically fully grown and were impacted in the bone, while the roots of deciduous teeth were not absorbed in patients II 3 (A) and II 2 (B), and the supernumerary teeth were located in the bilateral premolar regions in II 3. Narrow ascending ramus, with near parallel-sided anterior and posterior borders in patients II 2 and II 3; (C, D) Craniofacial radiograph showing underdeveloped maxilla and nasal bone, wormian bones in the occipital bone (II 3); (E-G) Radiograph showing hypoplastic clavicles and brachydactyly (II 3).

ported by the clinical phenotype and radiographic findings.

#### Identification of Runx2 mutations

All coding exons of the RUNX2 gene were successfully amplified by PCR using corresponding exon-specific primers. A novel base deletion mutation in exon 7 within the NMTS domain of RUNX2 (c.1271delC) was detected in the 29-year-old male proband, which caused a mis-

takenly-translated histidine from the 424<sup>th</sup> proline and introduced a novel stop codon at codon 483<sup>th</sup>, resulting in the loss of 39 amino acids (Figure 4A, 4D, 4E). The same mutation was detected in the other two affected individuals in this family. No mutations were detected in unaffected family members (Figure 4B) or in the 200 healthy controls (Figure 4C). I-TASSER indicated that the 1271delC mutation changed the tertiary structure, causing loss of parts of the beta turn and enfolded structure (Figure

## A novel mutation of RUNX2 in a Chinese family

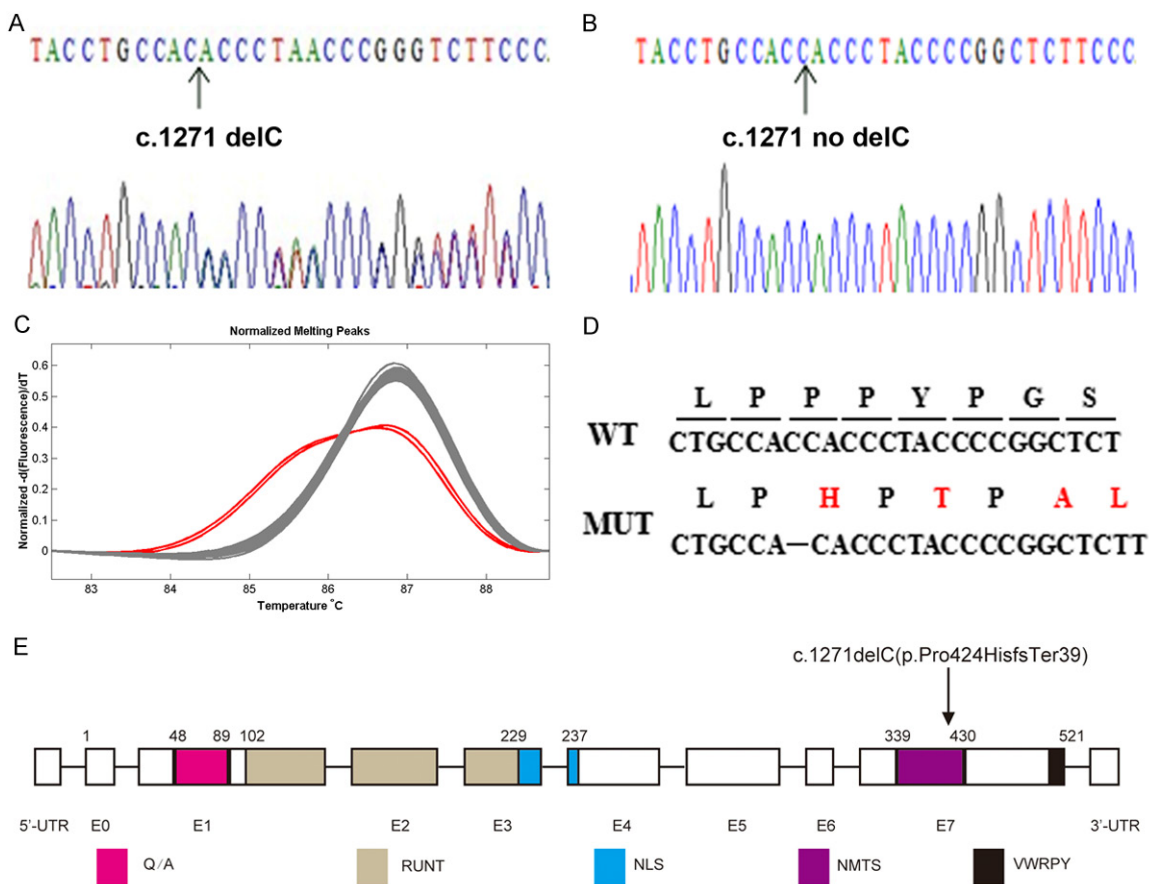


**Figure 4.** Mutational analysis of exon 7 of *Runx2*. A. Sequences from the proband, which show a new mutation (c.1271delC) in the NMTS domain; B. Sequence from the proband's son; C. Population screening, the red melting curve indicates individuals with CCD and the gray melting curve indicates healthy controls. The melting peaks of the former are lower than the latter; D. Amino acid sequences of wild-type and mutated *RUNX2*. Red indicates the amino acid differences between mutated and wild-type; E. A schematic showing functional domains and the mutation site (c.1271delC) identified in the present study. QA, glutamine and alanine repeats; RUNT, runt domain; NLS, nuclear localization; NMTS, nuclear matrix targeting signal.

5A) and Mutation Taster predicted that the mutation would be disease causing because the mutation changed the splice site and might affect protein features, including reduced DNA binding, impaired phosphorylation and impaired interaction with KAT6B.

### Functional analysis of mutant *RUNX2*

We found differences in the localization of wild-type and mutant protein. The subcellular localization of wild-type and mutant protein was assayed in HEK T 293 cells. The wild-type fusion protein was located in the nucleus, while the mutant fusion protein exhibited a different subcellular localization, being found both in the nucleus and the cytoplasm (Figure 5B). We extracted the RNA from affected and unaffected

family members, but did not find any obvious difference in mRNA expression of *Runx2* between them (Figure 5C). *In vitro*, we found significantly increased expression of the mutant protein compared to the wild-type protein. An identically sized band (~79 kDa) was observed from cells expressing the GFP-tagged wild-type *RUNX2* fusion protein. The mutant fusion protein showed a 74 kDa band (Figure 5D, 5E).

### Discussion

In our patients with the typical CCD phenotype, we identified a new frameshift mutation (P424HfsTer39) in exon 7 of the *Runx2* gene which caused the early termination of protein translation in the NMTS region. Due to the insufficient quantity of expressed *RUNX2* pro-

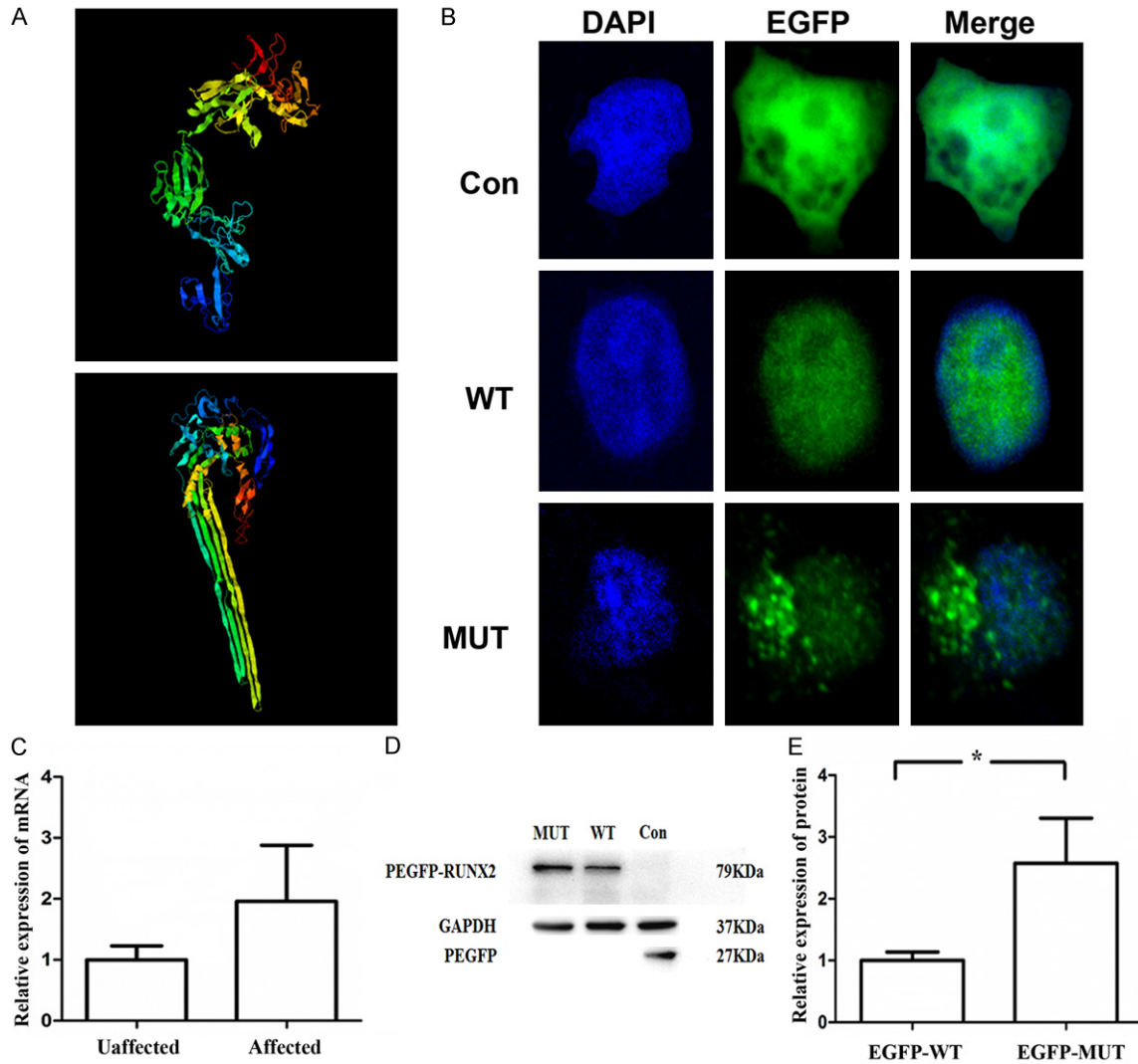


**Figure 5.** Functional study of the mutated protein. A. Predicted protein structure: wild-type (upper) and mutant (lower) by I-TASSER. B. HEK 293 T cells with subcellular localization of wild-type and mutant RUNX2. C. No significant difference in mRNA expression was seen between unaffected and the affected family members ( $P > 0.05$ ). D. Wild-type and mutant protein analyzed by western blotting. HEK 293 T cells transfected with GFP-tagged wild-type RUNX2 gave a 79 kDa band; the EGFP-fusion truncated mutant gave a 74 kDa band. EGFP, 27 kDa; GAPDH 37 kDa. E. There was a distinct difference in protein expression between wild-type and mutant RUNX2 protein ( $P < 0.05$ ).

tein, the phenotypic characteristics of patients may be caused by haploinsufficiency. Taking into account that the proband's father were clinically evaluated and his father has showed phenotypic characteristic of CCD, the proband and his elder sister's P424HfsTer39 mutations were probably inherited from their father.

The phenotypic spectrum of CCD patients ranges from mildly-affected individuals with only dental abnormalities to severely affected patients with generalized osteoporosis that is increased by immunosuppressive drugs [17].

However so far, there are few reports about the relevance of genotype/phenotype of CCD. Zhou *et al.* [18] found that the change in the RHD and PST region of the RUNX2 will cause the variable function loss of protein, which brings about different phenotypes including classic CCD, isolated abnormalities of teeth, and mild CCD. The clinical and radiographic manifestations of our cases seemed to be typical of CCD, including hypoplastic clavicles, short stature, underdeveloped maxilla and nasal bone, wormian bones, supernumerary teeth, retention of deciduous teeth, eruption failure of permanent

## A novel mutation of RUNX2 in a Chinese family

teeth and multiple malocclusions. Many studies have reported that in the NMTS region, insertion, deletion, or missense mutations leading to a translational stop codon in the C-terminal transactivating region, have caused typical CCD [12, 17, 19, 20]. Therefore, our study also provides bases for the study of the relevance between the genotype and phenotype of CCD.

Exons 1, 2, 3, and 7 of the *Runx2* gene encode three important functional domains of the protein: Q/A, RHD and PST. The mutation detected in this family in our study, c.1271delC, is located in the NMTS region (located in the middle of the PST domain) encoded by exon 7 of *Runx2*. The mutation resulting in heterozygous deficiency causes a frameshift of the nucleotide sequence in NMTS and failure of the encoded transcription factor to interact with Smads and other accessory proteins, thus resulting in incomplete transcriptional activation. In the process of osteogenesis, the transforming growth factor- $\alpha$  (TGF- $\alpha$ ) and bone morphogenetic protein (BMP) are of great importance, and Smads are critical mediators in TGF- $\alpha$ /BMP signaling [21]. Zhang *et al.* [16] detected a heterozygous C-to-T transition in exon 7 in a Japanese CCD patient, which resulted in a truncated RUNX2 protein, severely impairing RUNX2 transactivation activity. Due to failure in interacting with Smads, the osteoblast-like phenotype cannot be induced by truncated RUNX2 protein [22]. In promoting bone mineralization by hydrolyzing pyrophosphate, alkaline phosphatase (ALP) is a key factor expressed by osteoblasts. Previous studies have indicated that the recognition/binding and activation of ALP by RUNX2 are dependent on its targeting of the nuclear matrix [23]. Abnormality of NMTS, disrupting the Smad binding domain, affects the transcriptional activity of the *Alp* gene, and hinders the development of osteoblasts in patients which causes CCD.

Via *in vitro* testing, we found that the nuclear localization function changed in the mutant protein. The expression of green fluorescent protein (GFP) was not only detected in the nucleus but also in the cytoplasm. Although the NMTS plays an important role in the subcellular localization of RUNX2 protein, one or several mutations in the NLS domain located in the overlapping domain of RHD and PST domain,

the G159 [24] of RHD, the 93-158 aa [25] and 19-142 aa regions [26] of the N-terminus in the RHD, and 272-502 aa domain [27] of the C-terminus in the RHD will differently affect the subcellular localization of the protein. Unless all the components are mutated, the nuclear localization messages are not lost completely, so some of the GFP of the wild type can be detected in the nucleus. The last five highly-conserved amino acids of the C-terminal end comprise the VWRPY motif (**Figure 4E**) with which TLE/Grg interacts to inhibit RUNX2 transcriptional activity [28, 29]. In our study, we detected a deletion mutation in the last exon of the *Runx2* gene, resulting in a truncated RUNX2 protein. Consequently, the truncated protein will lack a part of the NMTS domain and the whole VWRPY domain. Due to the loss of transcriptional inhibition of VWRPY, the transcriptional activity of RUNX2 is enhanced, which results in higher protein expression of the mutant RUNX2. To our surprise, there was no significant difference between affected and unaffected family members in the mRNA expression of *Runx2*, but we found a tendency to increased mRNA expression of *Runx2* in the affected individuals (**Figure 5C**). The reason for the inconsistencies in the expression levels of protein and mRNA may be due to the reason that various and complicated posttranscriptional modifications in the generation of protein from the mRNA so that we can not exactly predict the protein concentrations based on mRNA [30].

In this family, the deletion mutation 1271delC was detected in the *Runx2* gene of the three patients with CCD, while no mutations were detected in unaffected family members. In the analysis of another 200 healthy volunteers, this mutation was also not detected, which further testified that the *Runx2* gene was the causative gene. The change of amino acid sequence in the RUNX2 protein affected its 3-D spatial structure and consequently affected the stability of the protein itself, its nuclear localization function, and interactions with other proteins, affecting the normal physiological function of the RUNX2 protein and causing the CCD.

### Conclusion

In summary, we have detected a novel single-base deletion mutation in exon 7 of the *Runx2*

gene of the proband. This will result in an amino acid change at codon 424 (P424H), and the introduction of a translational stop codon at codon 483. The functional analysis of the novel mutation was performed to illustrate the influence of haploinsufficiency and pathogenic mechanism of CCD, and it will expand our knowledge about the CCD pathogenesis and contribute to the molecular diagnosis of CCD.

### Acknowledgements

We thank the family members for their participation in the study. This work was supported by the National Natural Science Foundation of China (81371137) and Science and Technology Program of Guangzhou (201707010301).

### Disclosure of conflict of interest

None.

**Address correspondence to:** Bu-Ling Wu, Department of Stomatology, Nanfang Hospital, College of Stomatology, Southern Medical University, 1838 Guangzhou Avenue North, Guangzhou 510515, China. Fax: +86 20-62787149; E-mail: bulingwu@smu.edu.cn; Fu Xiong, Department of Medical Genetics, School of Basic Medicine Sciences, Southern Medical University, 1838 Guangzhou Avenue North, Guangzhou 510515, China. Fax: +86 20-61648510; E-mail: xiongf@smu.edu.cn

### References

- [1] Mundlos S, Otto F, Mundlos C, Mulliken JB, Aylsworth AS, Albright S, Lindhout D, Cole WG, Henn W, Knoll JH, Owen MJ, Mertelsmann R, Zabel BU and Olsen BR. Mutations involving the transcription factor CBFA1 cause cleidocranial dysplasia. *Cell* 1997; 89: 773-779.
- [2] Mundlos S. Cleidocranial dysplasia: clinical and molecular genetics. *J Med Genet* 1999; 36: 177-182.
- [3] Lee B, Thirunavukkarasu K, Zhou L, Pastore L, Baldini A, Hecht J, Geoffroy V, Ducy P and Karsenty G. Missense mutations abolishing DNA binding of the osteoblast-specific transcription factor OSF2/CBFA1 in cleidocranial dysplasia. *Nat Genet* 1997; 16: 307-310.
- [4] Qin X, Jiang Q, Matsuo Y, Kawane T, Komori H, Moriishi T, Taniuchi I, Ito K, Kawai Y, Rokutanda S, Izumi S and Komori T. Cbfb regulates bone development by stabilizing Runx family proteins. *J Bone Miner Res* 2015; 30: 706-714.
- [5] Vimalraj S, Arumugam B, Miranda PJ and Selvamurugan N. Runx2: structure, function, and phosphorylation in osteoblast differentiation. *Int J Biol Macromol* 2015; 78: 202-208.
- [6] Fang CY, Xue JJ, Tan L, Jiang CH, Gao QP, Liang DS and Wu LQ. A novel single-base deletion mutation of the RUNX2 gene in a Chinese family with cleidocranial dysplasia. *Genet Mol Res* 2011; 10: 3539-3544.
- [7] Zhang CY, Zheng SG, Wang YX, Zhu JX, Zhu X, Zhao YM and Ge LH. Novel RUNX2 mutations in Chinese individuals with cleidocranial dysplasia. *J Dent Res* 2009; 88: 861-866.
- [8] Sakai N, Hasegawa H, Yamazaki Y, Ui K, Tokunaga K, Hirose R, Uchinuma E, Susami T and Takato T. A case of a Japanese patient with cleidocranial dysplasia possessing a mutation of CBFA1 gene. *J Craniofac Surg* 2002; 13: 31-34.
- [9] Yamachika E, Tsujigiwa H, Ishiwari Y, Mizukawa N, Nagai N and Sugahara T. Identification of a stop codon mutation in the CBFA1 runt domain from a patient with cleidocranial dysplasia and cleft lip. *J Oral Pathol Med* 2001; 30: 381-383.
- [10] Goseki-Sone M, Orimo H, Watanabe A, Hamatani R, Yokozeki M, Ohyama K, Kuroda T, Watanabe H, Miyazaki H, Shimada T and Oida S. Identification of a novel frameshift mutation (383insT) in the RUNX2 (PEBP2 alpha/CBFA1/AML3) gene in a Japanese patient with cleidocranial dysplasia. *J Bone Miner Metab* 2001; 19: 263-266.
- [11] Chen T, Hou J, Hu LL, Gao J and Wu BL. A novel small deletion mutation in RUNX2 gene in one Chinese family with cleidocranial dysplasia. *Int J Clin Exp Pathol* 2014; 7: 2490-2495.
- [12] Cunningham ML, Seto ML, Hing AV, Bull MJ, Hopkin RJ and Leppig KA. Cleidocranial dysplasia with severe parietal bone dysplasia: C-terminal RUNX2 mutations. *Birth Defects Res A Clin Mol Teratol* 2006; 76: 78-85.
- [13] Zaidi SK, Javed A, Choi JY, van Wijnen AJ, Stein JL, Lian JB and Stein GS. A specific targeting signal directs Runx2/Cbfa1 to subnuclear domains and contributes to transactivation of the osteocalcin gene. *J Cell Sci* 2001; 114: 3093-3102.
- [14] Young DW, Zaidi SK, Furcinitti PS, Javed A, van Wijnen AJ, Stein JL, Lian JB and Stein GS. Quantitative signature for architectural organization of regulatory factors using intranuclear informatics. *J Cell Sci* 2004; 117: 4889-4896.
- [15] Harrington KS, Javed A, Drissi H, McNeil S, Lian JB, Stein JL, Van Wijnen AJ, Wang YL and Stein GS. Transcription factors RUNX1/AML1 and RUNX2/Cbfa1 dynamically associate with stationary subnuclear domains. *J Cell Sci* 2002; 115: 4167-4176.
- [16] Zhang YW, Yasui N, Kakazu N, Abe T, Takada K, Imai S, Sato M, Nomura S, Ochi T, Okuzumi S, Nogami H, Nagai T, Ohashi H and Ito Y. PEB-

## A novel mutation of RUNX2 in a Chinese family

- P2alpha/CBFA1 mutations in Japanese cleidocranial dysplasia patients. *Gene* 2000; 244: 21-28.
- [17] Lo ML, Tete S, Mastrangelo F, Cazzolla AP, Lacaita MG, Margaglione M and Campisi G. A novel mutation of gene CBFA1/RUNX2 in cleidocranial dysplasia. *Ann Clin Lab Sci* 2007; 37: 115-120.
- [18] Zhou G, Chen Y, Zhou L, Thirunavukkarasu K, Hecht J, Chitayat D, Gelb BD, Pirinen S, Berry SA, Greenberg CR, Karsenty G and Lee B. CBFA1 mutation analysis and functional correlation with phenotypic variability in cleidocranial dysplasia. *Hum Mol Genet* 1999; 8: 2311-2316.
- [19] Lee KE, Seymen F, Ko J, Yildirim M, Tuna EB, Gencay K and Kim JW. RUNX2 mutations in cleidocranial dysplasia. *Genet Mol Res* 2013; 12: 4567-4574.
- [20] Wang GX, Ma LX, Xu WF, Song FL and Sun RP. [Clinical and image features, and identification of pathogenic gene mutation of two cleidocranial dysplasia families]. *Zhonghua Er Ke Za Zhi* 2010; 48: 834-838.
- [21] Derynck R, Zhang Y and Feng XH. Smads: transcriptional activators of TGF-beta responses. *Cell* 1998; 95: 737-740.
- [22] Zhang YW, Yasui N, Ito K, Huang G, Fujii M, Hanai J, Nogami H, Ochi T, Miyazono K and Ito Y. A RUNX2/PEBP2alpha A/CBFA1 mutation displaying impaired transactivation and Smad interaction in cleidocranial dysplasia. *Proc Natl Acad Sci U S A* 2000; 97: 10549-10554.
- [23] Weng JJ and Su Y. Nuclear matrix-targeting of the osteogenic factor Runx2 is essential for its recognition and activation of the alkaline phosphatase gene. *Biochim Biophys Acta* 2013; 1830: 2839-2852.
- [24] Xuan D, Li S, Zhang X, Lin L, Wang C and Zhang J. A novel RUNX2 mutation in cleidocranial dysplasia patients. *Biochem Genet* 2008; 46: 702-707.
- [25] Lu J, Maruyama M, Satake M, Bae SC, Ogawa E, Kagoshima H, Shigesada K and Ito Y. Subcellular localization of the alpha and beta subunits of the acute myeloid leukemia-linked transcription factor PEBP2/CBF. *Mol Cell Biol* 1995; 15: 1651-1661.
- [26] Kim HJ, Nam SH, Kim HJ, Park HS, Ryoo HM, Kim SY, Cho TJ, Kim SG, Bae SC, Kim IS, Stein JL, van Wijnen AJ, Stein GS, Lian JB and Choi JY. Four novel RUNX2 mutations including a splice donor site result in the cleidocranial dysplasia phenotype. *J Cell Physiol* 2006; 207: 114-122.
- [27] Kanno T, Kanno Y, Chen LF, Ogawa E, Kim WY and Ito Y. Intrinsic transcriptional activation-inhibition domains of the polyomavirus enhancer binding protein 2/core binding factor alpha subunit revealed in the presence of the beta subunit. *Mol Cell Biol* 1998; 18: 2444-2454.
- [28] Levanon D, Goldstein RE, Bernstein Y, Tang H, Goldenberg D, Stifani S, Paroush Z and Groner Y. Transcriptional repression by AML1 and LEF-1 is mediated by the TLE/Groucho corepressors. *Proc Natl Acad Sci U S A* 1998; 95: 11590-11595.
- [29] Aronson BD, Fisher AL, Blechman K, Caudy M and Gergen JP. Groucho-dependent and -independent repression activities of Runt domain proteins. *Mol Cell Biol* 1997; 17: 5581-5587.
- [30] Greenbaum D, Colangelo C, Williams K and Gerstein M. Comparing protein abundance and mRNA expression levels on a genomic scale. *Genome Biol* 2003; 4: 117.